

NANO EXPRESS

Open Access

Combination of inverted pyramidal nanovoid with silver nanoparticles to obtain further enhancement and its detection for ricin

Meng Wang¹, Bin Wang¹, Shixuan Wu¹, Tingke Guo¹, Haoyu Li¹, Zhaoqing Guo¹, Junhua Wu², Peiyuan Jia², Yuxia Wang², Xiaoxuan Xu^{1*}, Yufang Wang¹ and Cunzhou Zhang¹

Abstract

We have obtained the surface-enhanced Raman scattering substrate by depositing silver nanoparticles on the surface of the inverted pyramidal nanovoid in order to improve the enhance effects. Experimental results showed that the combined substrate exhibited greater enhancement than the nanovoid substrate or nanoparticles. In order to test the SERS activity of the combined substrates, Rh6G and ricin toxin were used as Raman probes. Finite element method was employed to simulate electric field and induced charge distribution of the substrates, which have been used to explore the interaction between nanoparticles and nanovoid as well as mechanism of the great enhancement.

Keywords: Surface-enhanced Raman scattering; Ricin toxin; Combined substrate; Finite element method

PACS numbers: 73.20.Mf, 74.25.nd, 81.07.-b

Background

As the discovery of surface-enhanced Raman scattering (SERS) phenomenon [1,2], researchers have been working on the enhance mechanism, improvement, and practical applications. During the past several decades, it has been a fruitful research area and promoted Raman spectra to join the ranks of single molecule detection [3,4]. Nowadays, the huge enhanced factor is generally considered to be the result of two kinds of enhancements: one is the electromagnetic contribution (EM enhancement) which arises from the surface plasmon oscillation; the other is the chemical enhancement which involves chemical bonding and charge transfer. Moreover, the EM enhancement is considered to play a major role [5,6].

Based on the synthesis methods, there are two kinds of SERS substrates, nanostructures and nanoparticles (NPs), both can localize the optical energy into nanoscale and get field enhancement. To benefit from the nanofabrication techniques, various metallic plasmonic nanostructures have been manufactured and used as the

enhance substrates, such as bowtie and X-shaped nanostructures [7,8], truncated spherical nanocavities [9], Klarite substrate [10], sub-10-nm gap structure [11] nanomushroom and nano-ring arrays [12,13], and so forth. Noble metal nanoparticles of different shapes, dimensions, and compositions including the typical spherical, cubic [14,15], prismatic nanoparticles [16], 'sea-urchin'-like particles [17], spiky nanoshells [18], and Ag-Fe₃O₄ nanocomposites [19] have been synthesized and utilized in SERS. Here, we demonstrate that the further enhancement, which is stronger than solitary nanostructure or nanoparticles, can be obtained by combining nanostructures with nanoparticles.

With the advancement of SERS technique, researchers are not satisfied with the detection of routine analytes such as pyridine, rhodamine, and benzene thiol; instead, they utilize SERS in more wide applications for sensing molecules in trace amounts within the field of chemical and biochemical analytics, such as detecting DNA molecule [20], bacteria [21], cocaine, heroin [22,23], and explosives [24]. We have detected and distinguished a kind of phyto-toxin, ricin, using our combined SERS substrate. Compared with other detection method, such as enzyme-linked immunosorbent assay (ELISA) [25], SERS can identify the toxin rapidly with only a small amount of sample.

* Correspondence: xuxx@nankai.edu.cn

¹The MOE Key Laboratory of Weak Light Nonlinear Photonics, School of physics and Teda Applied Physics Institute, Nankai University, Tianjin 300071, China

Full list of author information is available at the end of the article

Methods

Substrate fabrication

Silver nitrate (AgNO_3 , 99 + %), poly(vinyl pyrrolidone) (PVP), and ethanol were purchased from Tianjin Jiangtian Chemical. Co. and used as received without further purification. Deionized water was prepared by a Milli-Q academic H_2O purification system and used throughout the experiment.

The nanostructure substrates used in this study were fabricated from (100) oriented silicon wafers. As shown in Figure 1b,c,e, after defining arrays of apertures by electron-beam lithography (EBL) on Cr mask, anisotropic KOH etching to the {111} planes and removing the mask, the inverted pyramidal nanovoid arrays were formed (Figure 1e). Apex angle of the nanovoid was fixed at 70.5° [26]. By adjusting etching time, the depth of the nanovoid can be controlled. A layer of gold with thickness of 200 nm was sputtered onto it. Scanning electron microscope (SEM) images of the inverted pyramidal nanovoid substrate are shown in Figure 2a,b.

The silver nanoparticles were prepared by solvothermal method [27]. First, 0.017 g silver nitrate was dissolved in 10 ml ethanol. After stirring it completely, the solution was injected drop by drop using a syringe into 20 ml ethanol which contains 0.3 g PVP (K-30). The mixed solution was transferred into Teflon-lined stainless autoclaves and kept at 180°C in drying oven for 18 h. Then, it was cooled naturally to room temperature and centrifuged. The supernatant was removed, and the precipitate was dispersed in deionized water and centrifuged again. After repeating the process three times, the silver colloid was obtained.

As demonstrated by the SEM images in Figure 2c,d, the prepared silver colloid mainly consists of nanospheres and nanorods. The diameter of nanosphere is about 80 nm, and the length of nanorod is about 140 nm.

The combined substrate of gold-inverted pyramidal nanovoids and silver nanoparticles was prepared by electrostatic assembly method, in which the silver colloid was dropped onto the gold substrate and dried naturally. The SEM images of the combined substrate in Figure 2e,f show that most silver nanoparticles distribute in the voids, especially around the slope edge. Compared with that on the silicon wafer, the distribution of Ag NPs is denser.

SERS experimental details

Rhodamine 6G (Rh6G) was used to characterize the SERS performance of the gold nanovoid, silver colloid, and combined substrate. 10^{-5} M Rh6G solution was chosen so that SERS signal could be obtained for all the three substrates under the same experimental condition. Rh6G solution was dropped onto the gold nanovoid or combined substrate. For the silver colloid enhancement, equivalent volume of colloid and Rh6G solution was mixed and dropped onto the surface of a polished silicon wafer. Raman spectra were collected by Renishaw confocal microscope Raman spectroscopy with 785-nm wavelength laser as an excitation source. The laser was focused on the substrates by a long working distance objective ($\times 50$ and $\text{NA} = 0.5$). The diameter of the focused laser beam is about $2\ \mu\text{m}$, and the power is 0.15 mW. The accumulation time is 10 s. For each enhanced substrates, six different points were randomly chosen to collect SERS spectra.

Theoretical simulation details

Finite element method (FEM) [28] was employed to simulate electric field and induced charge distribution of gold nanovoid substrate, silver nanoparticle dimer, and combined substrate. Linearly polarized plane wave was used as the incident source. Perfect match layers (PMLs) were applied in propagation direction to avoid nonphysical

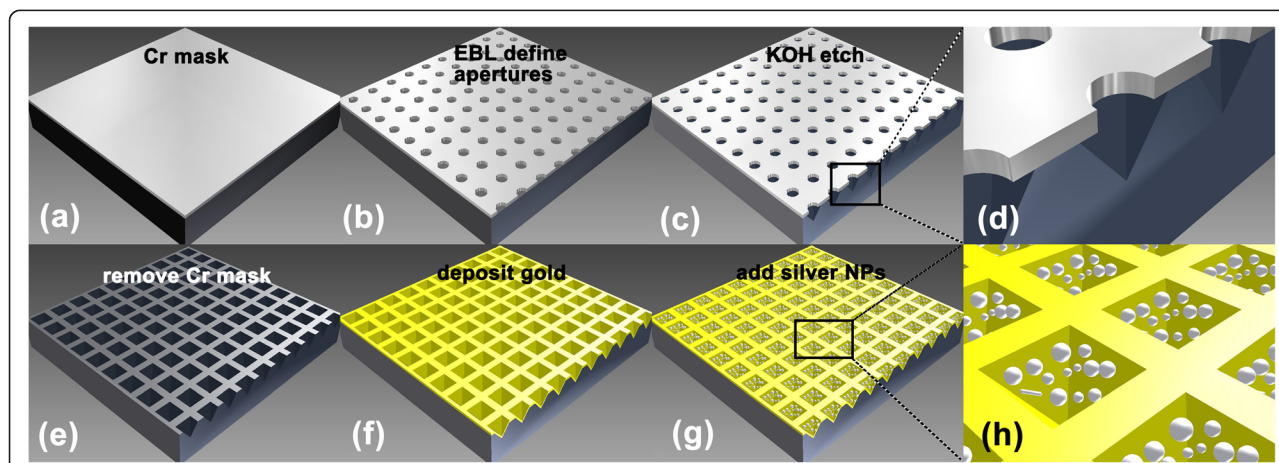


Figure 1 Nanostructure substrate fabrication process. (a) Deposit a layer of Cr on (100) oriented silicon wafer. (b) Define arrays of apertures on Cr mask by EBL. (c) Anisotropic KOH etching. (e) Remove Cr mask. (f) Deposit 200nm thick gold film. (g) Drop silver colloid onto the substrate. **d** and **h** are zoomed from **c** and **g**, respectively.

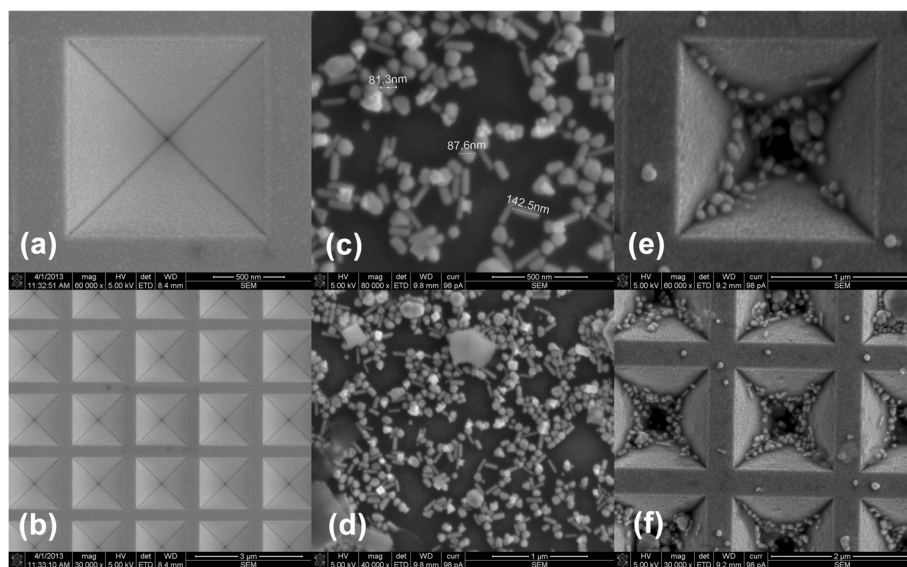


Figure 2 SEM images of prepared samples. **a** and **b** are SEM images of the inverted pyramidal nanovoid substrate. The pithead boundary length of the nanovoid is about 1.41 μm , its depth 1 μm , and its period 2 μm . **c** and **d** are SEM images of the prepared silver nanoparticles by solvothermal method. **e** and **f** are SEM images of the combined substrate.

reflection from boundaries. Periodic boundary conditions in x and y direction were used when simulating nanovoid substrate and combined substrate. The permittivity of gold and silver was referred to the experimental data of Johnson and Christy [29] and interpolated to get the dispersion relation.

Results and discussion

SERS spectra of Rh6G and ricin toxin

A comparison of SERS spectra of Rh6G obtained from three types of substrates is illustrated in Figure 3a. It can

be seen that the combined substrate demonstrates significant further enhancement. The scattering peak at $1,507\text{ cm}^{-1}$ is selected to compare the enhance performance. The peak area calculated from each spectrum is shown in Figure 3b. The average peak area obtained by combined substrate is about 44 times larger than that obtained by the solitary silver colloid and 107 times than that of the gold substrate.

In order to further investigate the enhancement effects of the combined substrate, SERS spectra of ricin with the concentration of 10 $\mu\text{g/ml}$ in phosphate-buffer saline

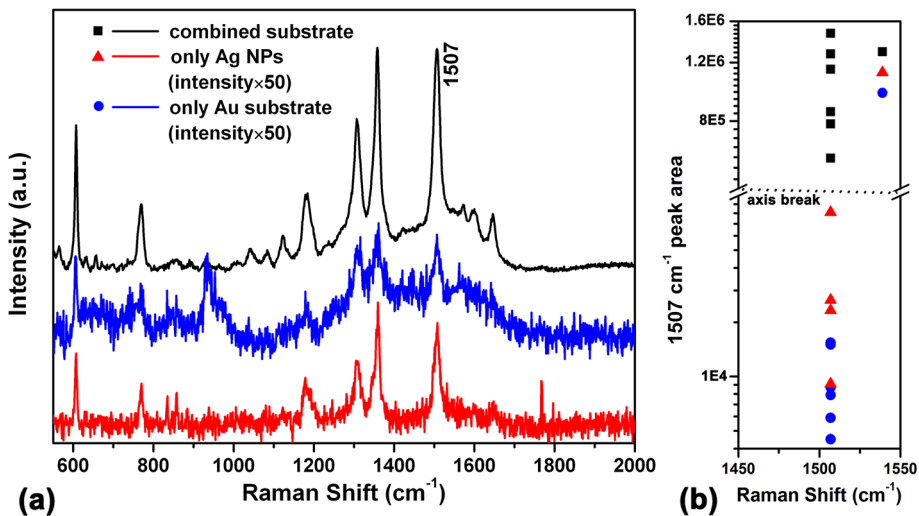


Figure 3 Comparison of SERS spectra of Rh6G. **(a)** Comparison of SERS spectra obtained by solitary gold nanovoid substrate, silver nanoparticles, and combined substrate. **(b)** $1,507\text{ cm}^{-1}$ peak area comparison. For visualization, a factor of 50 is multiplied to the spectra which correspond to gold substrate and silver nanoparticles in **a**, and the scale of vertical axis in **b** is taken logarithm.

(PBS) were measured. Ricin is a kind of toxin which can be easily extracted from castor seeds. Purified ricin with the size of a few grains of table salt could be fatal for an adult human. Ricin protein consists of two chains of polypeptide, A chain (RTA) bound to B chain (RTB) by a single disulfide bond. RTA can remove an adenine from ribosomal RNA (rRNA), prevent synthesis of protein, and cause the death of cells. RTB is a lectin that binds to glycoproteins or glycolipids on the surface of target cells and helps RTA penetrating into the cell [30].

In order to distinguish the Raman-scattered peaks of ricin from those of phosphate, Raman spectrum of phosphate solution was measured by dropping the solution onto the surface of the gold substrate. As shown in Figure 4a, the scattered peaks that appeared at 928, 1,060, and 1,125 cm^{-1} belong to phosphate, in agreement with the other report [31]. Another type of silver colloid, in which ethylene glycol instead of ethanol was chosen to reduce silver nitrate [32], was prepared to combine with the gold substrate. Raman spectra for naked combined substrate and ricin on the combined substrate were collected, as illustrated in Figure 4b-d. From Figure 4c, it can be seen that a new scattered peak which is distinguished from those of phosphate and the naked substrate appeared at 1,024 cm^{-1} . As can be seen from Figure 4d, a much stronger scattering peak at 1,024 cm^{-1} was obtained. Besides this major peak, other scattered peaks that appeared at 642 cm^{-1} and 1,209 cm^{-1} were also observed. These Raman bands are likely attributed to protein of ricin toxin.

Theoretical simulation results

In order to explore the mechanism of the further enhancement property of the combined substrate, finite element method was employed to simulate the near-field electric field distribution of the substrate under light illumination. E-field distributions of solitary gold nanovoid substrate and silver nanoparticle dimer were also calculated for comparison. As shown in Figure 5a,b,f, the plane wave which polarizes along the x -axis is incident from the top. The wavelength is 785 nm, which is the typical laser wavelength of Raman spectroscopy. The diameters of silver nanospheres in Figure 5b,f-i are 80 nm. The pithead boundary length of pyramidal nanovoid in Figure 5a,b is set to be 1.41 μm , depth 1 μm , and period 2 μm , in accordance with the size of the experimental substrate as shown in Figure 2. In Figure 5, all the gaps between nanoparticles or nanoparticle and nanovoid surface are 10 nm. The maximum of the color bar in Figure 5a,b,f is set to 10 V/m, which is convenient for comparison.

It can be easily observed from Figure 5b that there is a much stronger and larger area electric field distribution around the silver nanoparticles when combined with gold nanovoid. In this case, the maximum value of electric field intensity can be five times larger than that of the solitary gold nanovoid substrate or silver nanoparticle dimer. The large near-field enhancement can be explained by the double interaction between the combined substrate and incident light. First, the incident light is coupled into inverted pyramidal nanovoid. Then, the concentrated near fields in nanovoid have been further enhanced by silver

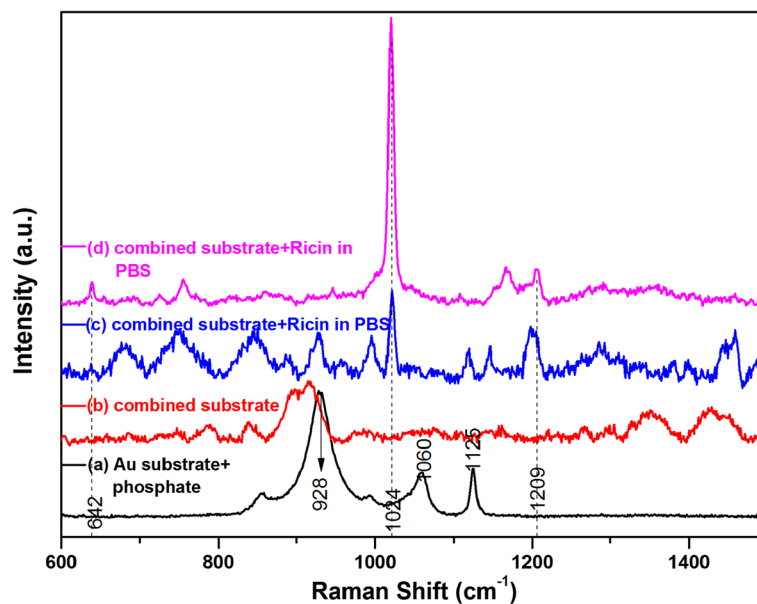


Figure 4 Distinguishing Raman signal of ricin toxin. Raman spectra collected from (a) phosphate on gold substrate, (b) combined substrate, and (c,d) ricin toxin in PBS on combined substrate.

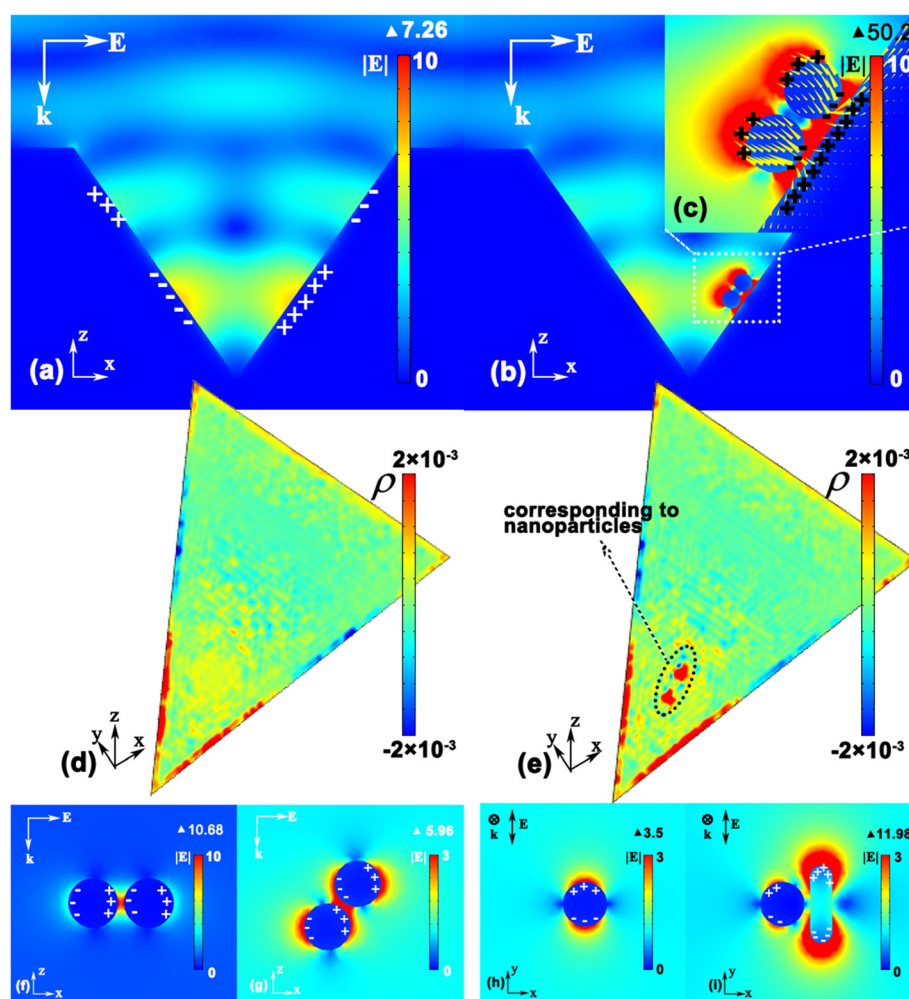


Figure 5 FEM-simulated field and charge distribution. Near-field electric intensity and induced charge distribution of (a) the periodic inverted pyramidal nanovoid, (b) combined nanostructure, (f) horizontally placed silver nanoparticle dimer, (g) obliquely placed dimer, (h) single silver nanosphere, (i) silver nanosphere, and nanorod. The tilt angles of silver dimer in b and g are the same. c is enlarged from b. d and e display induced charge density distribution on the surface of the nanovoid right side wall, corresponding to nanovoids shown in a and b, respectively.

nanoparticles, which result in a large near-field enhancement of combined substrate.

Schematic diagram of induced charge distribution is also plotted in Figure 5, from which we can observe that charge distribution is affected by the polarization of incident e-field and the interaction between metal nanoparticles. It can be observed from Figure 5g that the charge distribution of silver nanosphere has deviated from the polarization direction of incident e-field, due to the interaction of induced charges between two metal spheres. In the case of Figure 5b, because of the existence of nanovoid side wall, interaction between nanoparticle and the side wall becomes dominant. By comparing induced charge distribution on the surface of nanovoid right side wall with (Figure 5e) or without (Figure 5d) the silver nanoparticle dimer, it can be seen that nanoparticles play a role of

gathering charges. It is attributed to the appealing effect between charges on the surface of nanoparticles and nanovoid side wall. This effect causes accumulation of different charges on two sides of the gap, which promotes the oscillation of electron gas and its coupling with localized field, resulting in giant field enhancement.

In addition to the appealing effect of induced charges, there also exist the repelling effect due to the nanoparticle interaction, which is illustrated in Figure 5h,i. In Figure 5h, the induced charge distribution of a single silver nanosphere (diameter 80 nm) is consistent with polarization of incident e-field. When another metal nanoparticle (such as a silver nanorod, length 140 nm, diameter 40 nm) is placed very near to it, the 'hot areas' migrate further from nanorod obviously, which is due to the repelling effect of the same charges between nanosphere and nanorod.

Conclusions

We combined periodic gold nanovoid substrate with silver nanoparticles and obtained greater enhancement than solitary gold substrate or silver nanoparticles. SERS spectra were measured to characterize its enhancing property. Besides Rh6G, ricin toxin was also detected using the combined substrate. Theoretical simulation showed that much stronger and larger area electric field distribution, which was attributed to double interaction between the combined substrate and incident light, appeared around silver nanoparticles when combined with gold nanovoid. Induced charge distribution revealed the appealing or repelling effect between nanostructures.

Abbreviations

SERS: surface-enhanced Raman scattering; EM: electromagnetic; NPs: nanoparticles; ELISA: enzyme-linked immunosorbent assay; PVP: poly (vinyl pyrrolidone); EBL: electron-beam lithography; SEM: scanning electron microscope; Rh6G: rhodamine 6G; FEM: finite element method; PML: perfect match layer; PBS: phosphate-buffer saline; RTA: ricin A chain; RTB: ricin B chain.

Competing interests

The authors declare that they have no competing interests.

Authors' contributions

MW participated in the SERS experiment, performed the theoretical simulation, and drafted the manuscript. BW performed the nanovoid substrate fabrication and gold film evaporation. TG synthesized the silver nanoparticles. SW and ZG participated in the SERS experiment and SEM characterization. HL participated in the analysis of Raman spectra. JW, PJ, and Y(Yuxia) W provided the ricin toxin. XX and Y(Yufang) W conceived the study and supervised the work. Y(Yufang) W and CZ revised the manuscript and conducted coordination. All authors read and approved the final manuscript.

Acknowledgements

This work is supported by the National Science Fund for Talent Training in Basic Sciences (J1103208), Tianjin Science and Technology Supporting Project (12ZCZDZX02100), and the Marine Promotion Program from the Tianjin Oceanic Administration (KJXH2011-11). The authors also acknowledge the support from the Key Laboratory of Opto-Electronic Information Technology, Ministry of Education, Tianjin University, China.

Author details

¹The MOE Key Laboratory of Weak Light Nonlinear Photonics, School of physics and Teda Applied Physics Institute, Nankai University, Tianjin 300071, China. ²Institute of Pharmacology and Toxicology, Academy of Military Medical Sciences, Beijing 100850, China.

Received: 10 November 2014 Accepted: 6 February 2015

Published online: 28 February 2015

References

- Fleischmann M, Hendra PJ, McQuillan AJ. Raman spectra of pyridine adsorbed at a silver electrode. *Chem Phys Lett.* 1974;26:163–6.
- Jeanmaire DL, Van Duyne RP. Surface Raman spectroelectrochemistry: part I. Heterocyclic, aromatic, and aliphatic amines adsorbed on the anodized silver electrode. *J Electroanal Chem.* 1977;84:1–20.
- Nie S, Remory S. Probing single molecules and single nanoparticles by surface-enhanced Raman scattering. *Science.* 1997;275:1102–6.
- Kneipp K, Wang Y, Kneipp H, Perelman LT, Itzkan I, Dasari RR, et al. Field single molecule detection using surface-enhanced Raman scattering. *Phys Rev Lett.* 1997;78:1667–70.
- Campion A, Kambhampati P. Surface-enhanced Raman scattering. *Chem Soc Rev.* 1998;27:241–50.
- McNay G, Eustace D, Smith WE, Faulds K, Graham D. Surface-enhanced Raman scattering (SERS) and surface-enhanced resonance Raman scattering (SERRS): a review of applications. *Appl Spectrosc.* 2011;65:825–37.
- Hatab NA, Hsueh CH, Gaddis AL, Retterer ST, Li J, Eres G, et al. Free-standing optical gold bowtie nanoantenna with variable gap size for enhanced Raman spectroscopy. *Nano Lett.* 2010;10:4952–5.
- Wang D, Yu X, Yu Q. X-shaped quasi-3D plasmonic nanostructure arrays for enhancing electric field and Raman scattering. *Nanotechnology.* 2012;23:405201.
- Steuwe C, Kaminski CF, Baumberg JJ, Mahajan S. Surface enhanced coherent anti-Stokes Raman scattering on nanostructured gold surfaces. *Nano Lett.* 2011;11:5339–43.
- Hugall JT, Baumberg JJ, Mahajan S. Surface-enhanced Raman spectroscopy of CdSe quantum dots on nanostructured plasmonic surfaces. *Appl Phys Lett.* 2009;95:141111.
- Qi J, Li Y, Yang M, Wu Q, Chen Z, Wang W, et al. Large-area high-performance SERS substrates with deep gap controllable sub-10-nm gap structure fabricated by depositing Au film on the cicada wing. *Nanoscale Res Lett.* 2013;8:1–6.
- Shen Y, Zhou J, Liu T, Tao Y, Jiang R, Liu M, et al. Plasmonic gold mushroom arrays with refractive index sensing figures of merit approaching the theoretical limit. *Nat Commun.* 2013;4:2381.
- Liu H, Zhang X, Zhai T. Plasmonic nano-ring arrays through patterning gold nanoparticles into interferograms. *Opt Express.* 2013;21:15314–22.
- Wustholz KL, Henry AI, McMahon JM, Freeman RG, Valley N, Piotti ME, et al. Structure – activity relationships in gold nanoparticle dimers and trimers for surface-enhanced Raman spectroscopy. *J Am Chem Soc.* 2010;132:10903–10.
- McLellan JM, Siekkinen A, Chen J, Xia Y. Comparison of the surface-enhanced Raman scattering on sharp and truncated silver nanocubes. *Chem Phys Lett.* 2006;427:122–6.
- Wang Q, Song F, Lin S, Liu J, Zhao H, Zhang C, et al. Optical properties of silver nanoprisms and their influences on fluorescence of europium complex. *Opt Express.* 2011;19:6999–7006.
- Fang J, Du S, Lebedkin S, Li Z, Kruk R, Kappes M, et al. Gold mesostructures with tailored surface topography and their self-assembly arrays for surface-enhanced Raman spectroscopy. *Nano Lett.* 2010;10:5006–13.
- Hastings SP, Swanglap P, Qian Z, Fang Y, Park SJ, Link S, et al. Quadrupole-enhanced Raman scattering. *ACS Nano.* 2014;8:9025–34.
- Zhu S, Fan C, Wang J, He J, Liang E, Chao M. Realization of high sensitive SERS substrates with one-pot fabrication of Ag–Fe₃O₄ nanocomposites. *J Colloid Interf Sci.* 2015;438:116–21.
- He S, Liu KK, Su S, Yan J, Mao X, Wang D, et al. Graphene-based high-efficiency surface-enhanced Raman scattering - active platform for sensitive and multiplex DNA detection. *Anal Chem.* 2012;84:4622–7.
- Cheng IF, Chen TY, Lu RL, Wu HW. Rapid identification of bacteria utilizing amplified dielectrophoretic force-assisted nanoparticle-induced surface-enhanced Raman spectroscopy. *Nanoscale Res Lett.* 2014;9:1–8.
- Inscore F, Shende C, Sengupta A, Huang H, Farquharson S. Detection of drugs of abuse in saliva by surface-enhanced Raman spectroscopy (SERS). *Appl Spectrosc.* 2011;65:1004–8.
- Wei WY, White IM. Inkjet-printed paper-based SERS dipsticks and swabs for trace chemical detection. *Analyst.* 2013;138:1020–5.
- Botti S, Cantarini L, Palucci A. Surface-enhanced Raman spectroscopy for trace-level detection of explosives. *J Raman Spectrosc.* 2010;41:866–9.
- Chen HY, Tran H, Foo LY, Sew TW, Loke WK. Development and validation of an ELISA kit for the detection of ricin toxins from biological specimens and environmental samples. *Anal Bioanal Chem.* 2014;406:5157–69.
- Perney N, Baumberg JJ, Zoorob ME, Charlton MDB, Mahnkopf S, Netti CM. Tuning localized plasmons in nanostructured substrates for surface-enhanced Raman scattering. *Opt Express.* 2006;14:847–57.
- Yang Y, Matsubara S, Xiong L, Hayakawa T, Nogami M. Solvothermal synthesis of multiple shapes of silver nanoparticles and their SERS properties. *J Phys Chem C.* 2007;111:9095–104.
- McMahon JM, Henry AI, Wustholz KL, Natan MJ, Freeman RG, Van Duyne RP, et al. Gold nanoparticle dimer plasmonics: finite element method calculations of the electromagnetic enhancement to surface-enhanced Raman spectroscopy. *Anal Bioanal Chem.* 2009;394:1819–25.
- Johnson PB, Christy RW. Optical constants of the noble metals. *Phys Rev B.* 1972;6:4370.
- Audi J, Belson M, Patel M, Schier J, Osterloh J. Ricin poisoning: a comprehensive review. *Jama.* 2005;294:2342–51.
- Niaura G, Gaigalas AK, Vilker VL. Surface-enhanced Raman spectroscopy of phosphate anions: adsorption on silver, gold, and copper electrodes. *J Phys Chem B.* 1997;101:9250–62.
- Xing RM, An CX, Liu J. Preparation of silver nanoparticles via a solvothermal route. *Chemical Research.* 2001;5:63–5 (in Chinese).